Guide to the revised manuscript

This document begins by essentially duplicating our previously-submitted response to the comments of both reviewers (as before, our responses interlineated with their comments in indented ***bold italic type***). Portions of the response to comments in which we refer to changes made to the manuscript are highlighted.

This is followed by a copy of the revised manuscript with changes highlighted. In addition to changes made in direct response to reviewer comments, we also changed the units in which bulk concentrations were expressed to match those used internally in the CHROTRAN software and corrected a number of typos.

Comments of M. Walther (referee #1)

The manuscript describes the principles of a newly developed numerical model to simulate heavy metal contamination remediation involving biological fate (together with clogging) in saturated porous media; two example setups are provided to show the model's functionality. The approach is based on the open-source simulation toolbox PFLOTRAN and builds upon its functionality by extending the reactive module for the purpose of simulating the fate of heavy metals.

The structure of the manuscript is logically, providing an initial literature review, followed by a description of the used approach for the model development, before example calculations are presented. The manuscript is written in a clear and concise language; figures are used sparsely, tables summarize required model parameters; an appendix gives a short overview on the file structure for the newly developed features.

My view of the work is twofold. On the one hand, I highly support the publishing of new developments together with a proper benchmarking; this may at the first place not be acknowledged as a scientific advancement, but it very much provides the basis for the latter in many follow-up applications. This is furthermore highlighted by the fact that more and more approaches become increasingly complex which requires a proper documentation for a sustainable development of these approaches. In this light, I strongly support the publishing of this manuscript. On the other hand, I think that there is one major issue with the approach the manuscript presents. Heavy metal remediation is usually governed by the redox potential, which furthermore will change during the reaction and within biomass (biofilm). In the whole manuscript, I could not find any discussion or reasoning why you do not want to consider redox potential in your approach, which is so substantial for the whole reaction system. Having said this, I would like to raise the question whether the approach is sufficient for the broad applicability it claims to have (see page 3, line 30 ff). Also, the two examples only confirm the expected behaviour and cannot be used as benchmarks for the new processes. Therefore, I would like to encourage the authors to give reason 1) why it is ok to neglect redox potential, 2) why their approach is still capable to fulfil the expectations, and 3) provide appropriate benchmarks to ensure correct functioning of the new implementations.

I furthermore listed a number of specific comments below.

I hope that I could help to improve the manuscript and would be available for a second review, if the authors wish so.

> ***We thank the reviewer for taking the time to provide an objective, thorough review of the submitted manuscript, and for his overall positive comments. We have made a sincere effort to address their comments. With regard to the comments enumerated above:***
>
> ***1) Although calculation of redox potential helps to identify thermodynamically favorable reactions, the rates at which they will proceed vary significantly due to factors such as reaction overpotential and microbial enzymatic catalysis. In many cases, redox reactions are slow and redox-sensitive species may remain in thermodynamic disequilibrium (Keating and Bahr, 1998). For this reason, mathematical formulations of redox reactions, such as the model presented here, are often assumed to be kinetically limited, and are typically dependent upon the concentration of oxidant and/or reductant as opposed to the redox potential. This is justifiable because the concentration of the oxidant and/or reductant will have to approach exceedingly small concentrations before redox equilibrium is achieved (Steefel and MacQuarrie, 1996). Kinetic-partial equilibrium models have been implemented by others (e.g. McNab and***

Narsimhan, 1994; Keaton and Bahr, 1998). However, the calculation of redox potential or some other quantity describing electron availability is required. Thus, the redox-potential calculation brings additional parametric uncertainty and the resulting estimates will most likely not agree with field measurements of the electron activity (Eh). Numerous reactive transport models that incorporate biological and abiotic oxidation-reduction reactions for both reactions successfully take a kinetic approach (e.g. Hunter et al., 1998; Mayer et al., 2001, 2002; Li et al., 2009; Molins et al., 2015; Sengor et al., 2015;). Furthermore, this approach is beneficial because it allows the flexibility to calibrate the model using laboratory microcosms or field studies with relative ease. In the current system, it is known that the introduction of an organic carbon source such as molasses will result in reducing conditions, so reduction reactions are the primary driver of remediation. The following text was added to the manuscript (Section 2.2) "The governing equations include kinetically limited redox reactions. These reactions are often non-instantaneous with redox-sensitive species remaining in thermodynamic disequilibrium (Keating and Bahr, 1998), and a kinetic formulation is a fair representation of this type of behavior (Steefel and MacQuarrie, 1996)."

2) *In light of the above arguments, we believe that a "black box" kinetic approach without explicit treatment of redox potential is most suitable and flexible for the predictive modeling of a variety of heavy metals or other redox-sensitive contaminants for which CHROTRAN is intended.*

3) *We have added a suite of regression tests to the CHROTRAN repository, each of which illustrates the correct functioning of numerical solutions against analytical or empirical benchmarks. The included batch tests cover abiotic reaction, abiotic reaction with sorption (MIMT), microbial growth and decay, as well as interaction with biocide and nonlethal inhibitor. In addition a non-batch reference simulation featuring bio-clogging is included. These benchmarks are located in subdirectories of the* `chrotran_benchmarks` *directory in the developer branch (*`dev`*) of the CHROTRAN repository. In the top-level directory resides a bash script,* `chrotran_benchmarks.sh` *that runs them all. For behavior that is inherited from PFLOTRAN, no specific benchmarks are provided: we concur with the second reviewer that its validity is well established.*

References for the above citations:

Hunter, Kimberley S., Yifeng Wang, and Philippe Van Cappellen. "Kinetic modeling of microbially-driven redox chemistry of subsurface environments: coupling transport, microbial metabolism and geochemistry." Journal of Hydrology 209.1 (1998): 53-80.

Keating, Elizabeth Harrison, and Jean M. Bahr. "Reactive transport modeling of redox geochemistry: Approaches to chemical disequilibrium and reaction rate estimation at a site in northern Wisconsin." Water Resources Research 34.12 (1998): 3573-3584.

Li, Li, et al. "Mineral transformation and biomass accumulation associated with uranium bioremediation at Rifle, Colorado." Environmental science & technology 43.14 (2009): 5429-5435.

Mayer, K. Ulrich, David W. Blowes, and Emil O. Frind. "Reactive transport modeling of an in situ reactive barrier for the treatment of hexavalent chromium and trichloroethylene in groundwater." Water Resources Research 37.12 (2001): 3091-3103.

Mayer, K. Ulrich, Emil O. Frind, and David W. Blowes. "Multicomponent reactive transport modeling in variably saturated porous media using a generalized formulation for kinetically controlled reactions." Water Resources Research 38.9 (2002).

McNab, W. W., and T. N. Narasimhan. "Modeling reactive transport of organic compounds in groundwater using a partial redox disequilibrium approach." Water Resources Research 30.9 (1994): 2619-2635.

Molins, Sergi, et al. "A benchmark for microbially mediated chromium reduction under denitrifying conditions in a biostimulation column experiment." Computational Geosciences 19.3 (2015): 479-496.

Şengör, S. Sevinç, et al. "A reactive transport benchmark on modeling biogenic uraninite re-oxidation by Fe (III)-(hydr) oxides." Computational Geosciences 19.3 (2015): 569-583.

Steefel, Carl I., and Kerry TB MacQuarrie. "Approaches to modeling of reactive transport in porous media." Reviews in Mineralogy and Geochemistry 34.1 (1996): 85-129.

General

Please sort the variables by their occurrence in the equation.

We have made an effort to sort all variables as suggested.

For all variables explained, I suggest to use dimensions (LENGTH, TIME etc), not units (meter, seconds etc), whenever appropriate.

Although the use of dimensions would allow for a more generalized representation of the mathematical framework, we have elected to maintain the original representation in terms of units because they are consistent with how the equations are represented in the code itself. In particular, there is a hard-coded relationship between the units used for aqueous and bulk concentrations.

Introduction

The introduction nicely lists some published approaches for modeling heavy metal fate in saturated porous media. I understand that your literature study concluded that there was no sufficient model to fulfill the requirements listed in page 4, line 3 (btw: these achievement should rather be given in a summary at the end). I am wondering if you had any incentive to implement such a complex modeling approach (in other words: what was your motivation to develop such a new model)?

The primary motivation of developing this modeling approach was to simulate the remediation of legacy groundwater contamination at Los Alamos National Laboratory. Since the model is applicable to a wide range of contaminated sites, we have decided not to include our incentive for developing the model.

Page 3, Line 3: "t" is Time?

That is correct. This was added to the text.

Page 3, Line 3: I am wondering, whether the dimensions of the equation are correct (please correct me, if this is a wrong intension). The two left-hand side terms should have [MASS/VOLUME/TIME], but the right-hand side seems to have [MASS/VOLUME]. Can you explain this please?

Equations (1), (2), and (3) are proportional relationships and do not require consistent units, since they only represent a part of the entire governing equation. In this description, we are illustrating how various Monod expressions used by others influence ∂C/∂t and decided that writing the entire governing equations would unnecessarily add additional variables. The full governing relationship we use to define ∂C/∂t is written in Equation (11) and has consistent units [MASS/VOLUME/TIME]. The time dimension on the right-hand side of the expressions arises from the kinetic rate constants λ_C, Γ_{CD}, and the advection-dispersion operator.

Model description

P5, L11: What is L_b?

L_b represents a liter of bulk volume (i.e., total volume of a computational grid cell that includes both the porous medium and the solution), as opposed to a liter of pore water. A brief description of this unit was added to the manuscript.

P5, L11ff: many explained units seem to be concentrations, please state this in the bold names.

We believe that having the units written after the bold names as they were in the original submitted manuscript is sufficient. No changes were made.

P5, L26: - "...is the current porosity at LOCATION x"? - I assume, you define the porosity with 0 < theta < 1 relative to the total pore volume (ie. 1 - volume of solid phase)? - Why is it not D = D_i / theta(x,t) + D_m / (1 - theta(x,t))?

Dividing D_i by θ is necessary to express D_i in terms of solution volume as opposed to bulk volume. D_m is already written in terms of solution volume, so division by $1-\theta(x,t)$ is not required. In the revised manuscript, we have also added a 10^3 factor to the expression, which converts m^{-3} to L^{-1}.

P6, L4ff: q is not defined (you probably can write something like "with the water mass fluxes related to head via Darcy flux q")

We have modified the text to clarify this.

P6, L7ff: - theta is already defined on P5. - please revise the list of variables to use "and" and commas appropriately.

We have removed the redefinition of θ and revised the list of variables as suggested.

P6, L8: I suggest to move the note on additional capabilities of CHROTRAN to P5, L3, where you already give a small hint on additional features. Here, it seems not necessary to repeat this.

We have taken the reviewers advice and moved this description of additional capabilities to the beginning of the section.

P6, L23: I would like to discuss your statement, that you do not want to include the dispersive flux. I would argue that the distribution of the different components of the reactive system, ie. an aqueous contaminant, an electron donor, a biocide, is majorly governed by advection and hydrodynamic dispersion. With three (or more) governing components, the reactions should especially depend on the mixing of the fluid (and thus the solutes). However, you say that you do not want to consider mixing due to dispersion. Also, in biochemical applications, bacterial growth is usually limited by nutrient availability; growth of biomass often happens at the fringe of the biomass area (not talking about a biofilm here), while the inner areas will have a limited nutrient supply (as outer biomass has already used up all available nutrients). This, again is governed by (transverse) dispersivity and the mixing of the required constituents for biomass growth. Can you please elaborate on this? Besides the discussion on the relevance of dispersion, you sometimes speak of the "advection-dispersion operator" (eg P8, L12), which is somewhat misleading as you do not want to consider dispersion.

We agree with the reviewer regarding his scientific remarks about the importance of local-scale dispersion for mixing, and want to stress that CHROTRAN is capable of representing local-scale hydrodynamic dispersion. We did not choose to incorporate it in our examples because the relatively large block size implied non-trivial numerical dispersion and numerical mixing (all Eulerian reactive transport codes implicitly assume that reactants are uniformly distributed in the control volume). We expect the effects of local-scale dispersion to be minor by comparison, and would clutter the exposition. We now also remark explicitly that CHROTRAN does have the capability to handle general dispersion tensors.

P7, L12ff: I like fact that you describe the relevant biochemical processes (L11 says "chemical" processes). The mentioned assumptions, which you often state to be "common" or you assume to follow Monod or linear kinetics, however, should be backed up by a few references who did this in a similar way.

We made a sincere effort to describe the most common assumptions and approaches used to model heavy metal bioremediation in the introduction. For this reason, we do not feel the need to cite these works again. However, we did remove the statement "common assumption for bio-mediated processes" from the sentence describing the bio-reduction process.

P7, L27: A question of understanding: If biomass decays, e.g. through lysis, will this release the heavy metals again, or will other biomass be able to use this as nutrients?

It is possible that the heavy metal could be assimilated into cells during anabolism. In this case, the heavy metal would be released during lysis. However, enzymatic reduction of the contaminant could also occur extracellularly (e.g. through an electron shuttling process). Our model assumes that reduction is occurring as a dissimilatory reaction that occurs extracellularly, so biomass decay would not necessarily release the heavy metal. The contaminant would have to be re-oxidized prior to its utilization by other biomass.

P9, L1, Eq 11 ff: Maybe, I missed it, but what is S?

The variable S represents stoichiometric relationships between a reaction rate and the consumption rate of a certain species. The variable is defined in the first paragraph of Section 2.2 (Biogeochemical reactions).

P9, L10ff: Please add some references for the testing cases, benchmarks, and applications which PFLOTRAN is used for. Furthermore, I understand that your new implementation may be hard to test against other software that do not have the capability to run these setups. However, I think that you could have chosen examples that have the option to either neglect the new processes or to include them; for the former, you could run alternative models and test them against your implementation; for the latter, differences should be visible that should be validated against mass balances for consistence.

As per the reviewer suggestion, we have added multiple references for PFLOTRAN testing cases, benchmarks, and applications. In order to test our CHROTRAN implementation, we have added additional test problems which are not presented in the manuscript but are available in the developer branch (*`dev`*) of the CHROTRAN repository. We have added the following sentence to the manuscript. "Additional batch test problems can be found in the developer branch of the CHROTRAN repository (*`chrotran_benchmarks`* directory)." These new problems test the various capabilities of CHROTRAN individually in a batch simulator and compare the CHROTRAN numerical solution against analytical or empirical benchmarks implemented in Python. We feel that this additional effort provides compelling evidence that CHROTRAN is working as intended, and it overcomes the difficulty of comparing with other reactive transport models that rely on different conceptual models and mathematical formulations.

P10, L3: Where can I find the CHROTRAN repository? (Please add a reference to P12, L20.)

The CHROTRAN repository is located at `https://github.com/chrotran/release`***. Additionally, we have setup a CHROTRAN homepage that can be found at*** `http://chrotran.lanl.gov`***.***

P11, L4: What does the unit "M" stand for? Figure 2: - If t=400d, flow velocities at the well are very small (practically zero?) due to bioclogging. At this point, you start to inject a biocide. I have to questions: 1) As hydr. conductivity is very low, the distribution of the biocide should majorly be governed by diffusion. I am astonished that this relatively large area (~5x5m2) is remediated so fast. Can you explain this? 2) For all t>400d, the shape of the "remediated area" (where the biocide is injected) shows the shape of a diamond; why isn't this shape similar to the shape of the biomass? Is this a numerical artifact?

The unit M represents molar concentration (mol L^{-1}). We have changed the units to mol L^{-1} to maintain consistency throughout the text.

1) ***The hydraulic conductivity is indeed low enough for flow velocities to be practically zero at t=400 days given the pressure gradients induced by the ambient hydraulic gradient and injection. However, the specified kinetic rate constant, the high concentration of both biomass and biocide, and numerical mixing at the scale of the Eulerian control volumes results in the relatively fast destruction of biomass in the vicinity near the well. Careful inspection of the figure reveals a fringe area (light green) with intermediate biomass concentration around the region that has been completely unclogged (white). Transport in this region is indeed dictated by diffusion and slow advection. However, the combination of factors described above makes the transition from diffusion to advection controlled transport occur at a small enough time scale that the unclogged zone is able to propagate outwards.***

2) ***The reviewer is correct that this is a numerical artifact: in particular, the "concave diamond" remediated area has the shape that it does on account of numerical dispersion and the relatively coarse grid, whereas in reality should be near-circular. Essentially: numerical dispersion in the x and y directions is proportional to flow velocity through the grid faces that are respectively orthogonal to these directions. If we imagine that the true seepage velocity at the well has magnitude $|v|$, and an effective numerical dispersivity, α, applies in both x and y directions, it follows that the effective longitudinal dispersion in those directions is described by Fick's law constant $D = \alpha|v|$. However, for flow at 45 degrees to these axes, it is easy to see that the effective longitudinal dispersion is described by Fick's law constant $D = \frac{\alpha|v|}{\sqrt{2}}$, with dispersion strength in other directions lying between the two extremes. This accounts for the non-physical concave diamond shape near the well. This imperfection can be addressed by increasing the resolution near the well.***

   The reviewer also asked why the shape of the outer bound of the biomass was not the same shape as the interior bound. This is because the flow fields are qualitatively different at these locations. As the interior remediated region begins to develop, it is embedded in a region of thick biomass, and experiences no ambient flow, and so develops in a purely "radial" fashion. By contrast, the exterior of the biomass has ambient flow around its edges, somewhat analogous to the flow around an airplane wing. This flow streamlines the biomass and tends to fill concave regions that we might otherwise see (although note that these would slowly fill due to diffusion, anyhow). In the absence of ambient flow, the exterior of the biomass would have a more pronounced diamond shape, analogous to the remediated region.

Summary and conclusions

P11, L26: You did not show the three-dimensional capabilities of your code.

We replaced "three-dimensional" with "multi-dimensional" here and in the abstract.

P12, L4: You also did not show the HPC capabilities of your implementation.

We replaced "high-performance computing capabilities" with "existing capabilities".

Source Code

I could find the source code on github, but could not find any pull requests or commits that build upon the original PFLOTRAN code. Therefore, I could not check any of the new developments you implemented. I highly recommend, especially for further development of your code, to provide a repository that uses as an initial commit an unchanged PFLOTRAN version and then shows your additions as several, logically combined commits.

We apologize for the lack of revision history in our original source repository on GitHub. We agree with your suggestion and have updated the source code. The new CHROTRAN repository can be found at `https://github.com/chrotran/release`***. We have reorganized the repository into a development branch (***`dev`***) and a release branch (***`release`***). By default, release is the default branch. Running*** `git log` ***in the new repository will show that it maintains all of the change sets found in the*** `pflotran-dev` ***repository. This enables us to pull and merge changes from*** `pflotran-dev` ***to both the CHROTRAN release and dev branch and also maintain the simplicity of the original CHROTRAN repository that accompanied the manuscript submission. The latest release version of CHROTRAN possesses the tag*** `"v1.0"`***. Minor changes were made to the source code of this version that make it different from the source code submitted with the original manuscript (see the revision log for details). However, these changes were mainly cosmetic and do not change any of the original simulation results presented.***

Appendix

P12, L26: Please indicate the PFLOTRAN version you used as a base. Do you think you could easily rebase your code to a future release of PFLOTRAN?

CHROTRAN version 1.0 in the new GitHub repository is based upon `pflotran-dev` ***commit*** `8f33d80`***. This information, along with the required change set for PETSc (***`03c0fad`***) has been added***

to the manuscript. Reorganizing the GitHub repository will allow straightforward rebasing of our code to future releases of `pflotran-dev`***, as described above.***

P13, L28: please add reference to VisIt and ParaView. See this for the latter: https://www.paraview.org/publications/

These citations have been added.

Typos, Grammar, etc.

Page 3, Line 4: Please remove the comma in "where C, is the U(VI) concentration".

This has been corrected.

Later, C is also reused for other heavy metal concentrations, please mention that.

We have changed the wording to "where C is the heavy metal (U(VI)) concentration".

P10, L10: Please change meter to square meter.

This has been corrected.

P10, L12: epsilon, the initial concentration should have a unit.

We initially did not specify units because the units differ for aqueous and immobile phase concentrations. We have corrected the sentence to include appropriate units for all of the included species. This correction was also made to section 3.2 (biomass clogging case study).

P12, L24: "complier" -> "compiler"

This has been corrected.

Comments of anonymous referee #2

The manuscript "CHROTRAN 1.0: A mathematical and computational model for in situ heavy metal remediation in heterogeneous aquifers" by Hansen et al. (gmd-2017-51) presents a conceptual modeling approach for the reaction-transport simulation of chromium in groundwater. The conceptual approach considering, transport sorption, biotic and abiotic reduction of Cr(VI), growth and decay of microbial biomass, and clogging of the pore space due to biomass accumulation is implemented into the 3D reactive transport environment PFLOTRAN. The performance of the approach is demonstrated using two generic case studies.

The manuscript is well written and the presented approach appears in general technically sound making use of well-established concepts. Some of the assumptions regarding the considered processes and their kinetic description would need a better explanation/justification but my largest concern regarding this manuscript is whether it indeed presents a new model or whether is presents 'just' an application of PFLOTRAN for the simulation of Cr(VI). Given that the shown model applications are two generic scenarios without any in-depth discussion of the results and their potential meaning, it is not possible to validate the applicability of the presented conceptual approach (i.e. set of equations) to real-world scenarios. If – as I appears to me – the novel aspect of the manuscript is restricted to the conceptual approach it would not justify publication of the manuscript.

> ***We appreciate the reviewer's assessment of our approach as well written and generally technically sound. We have added some text to the revised manuscript to deal with a number of the reviewer's technical queries.***
>
> ***Regarding the main point of criticism: we stress that it is not correct that CHROTRAN is just an "application" of PFLOTRAN. In its stock form, PFLOTRAN is unable to model either the reaction kinetic equations that we developed, or the effect of bio-clogging. While PFLOTRAN's code is written in a modular way so that those who want to build upon it do not have to reinvent the wheel, substantial software development effort was required in order to build an executable that implements our novel functionality. We estimate that more than 100 man-hours were devoted to software development alone, apart from the conceptual model development and quality assurance, with well over a thousand lines of code added. Thus, the contribution we describe is the development of a new model, its full software implementation, and some example applications. This places our report well inside Geoscientific Model Development's "Model Description Paper" category.***

Specific comments:

P3, L28: Is the only short-coming of the existing models for Cr(VI) reduction the fact that they consider 1D transport only? If so, why is there a need for an alternative description of the reactive processes?

> ***This is not the only shortcoming relative to our model; we describe in detail how our model dynamics differ from existing bio-reduction models in the introduction. However, it is a major shortcoming of the models we discussed and we feel it is worth stressing.***

P4, L21: No, there are several other codes which would be capable of simulating the presented processes (perhaps not always the clogging, but certainly all the reactive processes). See e.g., Schäfer et al., 1998, Journal of Contaminant Hydrology 31: 167; Mayer et al., 2002, Water Resources Research 38: 1174; Prommer et al., 2003, Ground Water 41: 247; Centler et al., 2010, Computational Geosciences 36: 397. All these models would be sufficiently flexible to allow describing the presented processes using the set of equations shown further down in the manuscript.

> ***Even leaving aside the clogging, none of the four papers listed by the reviewer describe capability that is comparable to that which we have developed. Indeed, two of them (Mayer et al. and Prommer et al.) describe models that do not actually treat biomass dynamics explicitly. The other two papers do not include dynamics that we include here. We review all four papers in turn and show how their presented models differ from ours:***
>
> 1. ***Schäfer et al. (1998) present the model that is closest in spirit to our model, and explicitly treat biomass as a species. They specifically include a first-order mass transfer terms for electron donor and receptor movement between the biofilm and aqueous phase, which we***

do not. Our model features a more flexible biomass crowding inhibition term and also features the following behavior that was not included in Schäfer et al. (1998):

a. ***Feedback between biomass growth and permeability.***
b. ***Decay of biomass concentration back to a non-zero background level.***
c. ***Direct reaction between biocide and biomass.***
d. ***Possibility of consumption of electron donor which is proportional to biomass concentration rather than biomass growth.***

2. ***Mayer et al. (2002) present a sophisticated flexible reactive transport model for handling aqueous-phase and precipitation-dissolution reactions. However, as the authors themselves write: "[b]acterial growth and die-off is neglected in the present formulation." Microbial reduction can only be treated through use of Monod-type kinetic equations for aqueous species, and biomass concentration and growth rate cannot be factors in these equations.***

3. ***Prommer et al. (2003) discuss applications of the PHT3D model. In this paper, an example of bioremediation of chlorinated solvents is modeled, in which every reaction is treated as a first-order decay. Consultation of the PHT3D manual also shows an example in which the Monod and inhibition terms participate in the kinetic equations for aqueous species. No examples were found in which dynamics of immobile biomass concentrations were simulated.***

4. ***Centler et al. (2010) present the GeoSysBRNS model, which explicitly treats biomass concentration and discussed a bio-mediated $A + B \rightarrow C$ reaction; The biomass dynamics presented here were simpler than those shown in Schäfer et al. (1998), with first-order decay, linear dependence on biomass concentration, and Monod dependence on the concentrations of A and B. On the evidence of this paper and a 2013 follow-up which is the only other publication listed on the GeoSysBRNS website, the following features of CHROTRAN are not included:***

    a. ***Any sort of crowding-based biomass growth inhibition term.***
    b. ***Biomass growth inhibition by ethanol or other conservative species.***
    c. ***Feedback between biomass growth and permeability.***
    d. ***Decay of biomass concentration back to a non-zero background level.***
    e. ***Direct reaction between biocide and biomass.***
    f. ***Possibility of consumption of electron donor which is proportional to biomass concentration rather than biomass growth.***

While these papers do not describe models that are equivalent to ours, we have enhanced the literature review section to include the Schäfer et al. (1998) and Centler et al. (2010) papers, and thank the reviewer for this comment.

P5,L5-8: While I support this line of approach I am wondering why it would need an 'new' model for its simulation. What is presented in the following is the abiotic and biotic redox transformation of two (partially) mobile species. This is handled by quite a number of reaction-transport models for groundwater settings and it actually does not matter if the electron donor or the electron acceptor is considered as contaminant.

Without reiterating our response to the last question, our model contains a number of bio-reduction-specific features that are not found in other reactive transport models. In particular, we treat biomass explicitly, as an immobile species which occupies space and reduces permeability, which has a background concentration, governed by a hard-limiting biomass crowding term (with tunable exponent), and which can participate in metabolic, abiotic, and conservative inhibition interactions with aqueous species. Some codes may share some of these features, but no existing code has all of them.

P5, L11: It appears quite strange/confusing introducing B with the unit mol/L but then interpreting 1 mol as 1 g… Why not stating that the unit of B is up to the user and eventually requires the units of the parameter S_D to be defined consistently.

> ***Our argument for using this formulation is in the paragraph to which the reviewer refers, and we do state that the choice of what a "mol" represents is up to the user. We think it is important to show the denominator as a bulk volume, which might not be clear if we simply wrote "the choice of the unit of B is up to the user". Since some symbol would have to represent amount of biomass in the square bracketed unit expression, "mol" seems as good as any.***

P5, L26: This implies that the reactivity of the sorbed and the dissolved donor is the same. If this would be the general case, many researchers studying reductions of bioavailability due to sorption would waste their time. Some words of discussion/justification would be needed here.

> ***The reviewer is of course correct that the bioavailability of sorbed and aqueous species differ. However, as long as the sorbed and aqueous species are in quasi-local-equilibrium, it is possible to define an effective reaction rate constant for the total species. We have added text in the paper indicating this in response to this comment.***

P6,L12/Eq.6: In the literature one can find a large number of possible relations between changes of porosity and changes of hydraulic conductivity due to (bio)clogging. However, to my knowledge a linear relation has not been proposed, yet. Give reference/justification for this assumption.

> ***This approximation can be justified by the Zunker empirical formula [e.g., Morin, R.H. "Negative correlation between porosity and hydraulic conductivity in sand-and-gravel aquifers at Cape Cod, Massachusetts, USA." Journal of Hydrology 316 (2006): 43] which states that*** $K \propto \frac{\theta}{1-\theta}$***. From this, it follows immediately that***
>
> $$\frac{K(t)}{K(0)} = \frac{\theta(t)}{\theta(0)}\left[\frac{1-\theta(0)}{1-\theta(t)}\right].$$
>
> ***As long as*** $\theta(0)$ ***is sufficiently small, the square-bracketed term may be treated as unity, and the fractional reduction in permeability equal to the fractional reduction in porosity. We show below a numerical example in which an initial 25% porosity is reduced to zero, with the near linearity of the corresponding K as a function of*** θ***:***

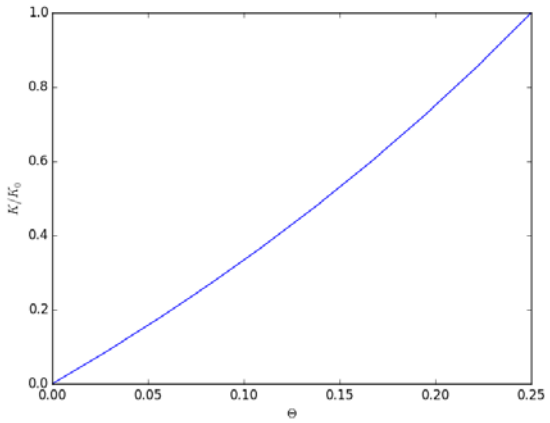

P8, L8/Eq.9 and P9, L1/Eq.11: Why is there no dependency of microbial growth on the contaminant/electron acceptor? This implies that everywhere some other (more favorable) electron acceptor must be available at non-limiting concentrations. If this would be the case why should there be a consumption of the heavy metal? Also, why is the bio-reduction rate not controlled by the presence of the electron donor? The equation implies that as long as there is sufficient biomass there would be a bioreduction activity even if the is no further supply of the electron donor. This does not appear meaningful to me.

We discussed our decision to neglect dependence on the electron acceptor in lines 21-29 on p. 3 of the original manuscript, and included references to modeling and experimental precedent. To elaborate: numerous processes may be involved in microbial heavy metal reduction: usage of the heavy metal as the terminal electron acceptor (TEA) in cellular respiration, incidental enzymatic reduction, and abiotic reduction by metabolites [Dhal, B., et al. "Chemical and microbial remediation of hexavalent chromium from contaminated soil and mining/metallurgical solid waste: a review." Journal of Hazardous Materials 150-151 (2013): 272]. Bio-reduction of Cr(VI) has been observed even under aerobic conditions in the subsurface [ibid], so it is overly restrictive to assume that the heavy metal will be restricted to the role of the TEA. We use a general approach to modeling the consumption of the heavy metal by the biomass, in which its rate of microbial consumption may be treated as an arbitrary linear combination of the biomass growth rate and biomass concentration. We believe that this should cover most field scenarios, except perhaps for some very specific experiments in which there is no TEA availability besides the single metal contaminant.

It has also been shown in batch experiments that cells which are grown with an electron donor, washed, and then placed in suspension with Cr(VI) and no energy source are still able to reduce the Cr(VI) to Cr(III). This so-called "endogenous respiration" has been described for a variety of metal-reducing scenarios [Fredrickson, J. K., H. M. Kostandarithes, S. W. Li, A. E. Plymale, and M. J. Daly. "Reduction of Fe(III), Cr(VI), U(VI), and Tc(VII) by Deinococcus radiodurans R1." Applied and Environmental Microbiology 66 (2000): 2006].

P9, L7/Eq. 15: Is there a process-related justification of the existence of B_min or has this been introduced for technical/numerical reasons?

B_{min} represents the background concentration of indigenous biomass that exists in the aquifer in the absence of bio-stimulation. Including B_{min} does provide a numerical benefit in that it prevents B from reaching exceedingly small values when no amendment is present, which could cause transport solver convergence issues. Exceedingly small concentrations of B could also prevent growth during the addition of an amendment, since the growth rate (μ_B) is a function of B.

P9, L12: No, there are other codes which could be used for this purpose (see comment above for P4, L21). However, I agree that benchmarking is not needed here. PFLOTRAN is well established and any benchmark would not allow determining if the presented concept is meaningful.

We reiterate that it is not true that other codes could be used for our governing equations, but agree that the reliability of the numerical solvers and I/O handling that we borrow from PFLOTRAN is well-established.

P9, L14: Are any of these validations available in the literature? If not this statement might of course be true but any evidence for this is lacking.

Nothing is currently available in the literature, as this is the first manuscript written regarding CHROTRAN. In light of both reviewers' comments regarding CHROTRAN benchmarking, we have now included regression test routines in the repository, which are accessible to all. We have added the following sentence to the manuscript. "Additional batch test problems can be found in the `dev` ***branch of the CHROTRAN repository (in the*** `chrotran_benchmarks` ***directory)." These new problems test the various capabilities of CHROTRAN individually in a batch simulator and compare the CHROTRAN numerical solution against analytical or empirical benchmarks implemented in Python. We feel that this additional effort provides compelling evidence that CHROTRAN is working as intended.***

P 10, L8: Clarify, are the parameters shown in Tables 1 and 2 those also shown in Figures A1 and A2. I support showing these figures to visualize how the case specific input has to be provided but for communicating parameter values a table is more appropriate. Also: where do these parameter values come from, literature, own experiments/studies, educated guess or…? What is the initial porosity (especially for the clogging case shown further down)?

We indicate that the exact input files used for both of our examples are available in the repository, and so to avoid redundancy we did not duplicate them in the manuscript: Figures A1-A3 are provided as user manual examples, only. In these examples, parameters are chosen for convenience and illustrative value. Although they are intended to be realistic, they are not based on any particular site or set of experiments. We agree that failing to indicate the initial porosity used for the clogging example was an oversight and we have corrected this.

P 11, L2: Is a constant head injection a reasonable assumption? Usually wells impose a certain flow rate. As there is no shear force related biomass removal considered I assume that the model would not predict reasonable effects for a fixed injection rate well.

CHROTRAN is capable of handling essentially arbitrary conditions at wells, including constant and time-variant head and constant and time-variant flow rates. We chose a constant-head boundary because it best illustrates the change in flow rate around the well due to bio-clogging. An imposed constant flow rate would (a) show no change in flow regime, and (b) be non-physical, since any pump has only finite ability to create a pressure differential, which would be eventually overcome as the permeability around the well dropped to zero.

P 11, L20: If the biomass seems to inhibit any injection through the well, the dithionite injection would not lead to any effects as long as the biomass is not decreasing due to natural decay allowing at least some injection to take place. Right?

From an engineering point of view, there is always a contact front between dithionite-containing pore water and biomass (and indeed some slow, irregular flow). So, it is not required in actuality for biomass to begin dying on its own for dithionite to be effective. From a numerical point of view, numerical mixing at the scale of the Eulerian control volumes ensures some "contact" between biomass and biocide.

CHROTRAN 1.0: A mathematical and computational model for in situ heavy metal remediation in heterogeneous aquifers

Scott K. Hansen[1], Sachin Pandey[1], Satish Karra[1], and Velimir V. Vesselinov[1]

[1]Computational Earth Science Group (EES-16), Los Alamos National Laboratory

Correspondence to: Scott K. Hansen (skh3@lanl.gov)

Abstract. Groundwater contamination by heavy metals is a critical environmental problem for which in situ remediation is frequently the only viable treatment option. For such interventions, a multi-dimensional reactive transport model of relevant biogeochemical processes is invaluable. To this end, we developed a model, CHROTRAN, for in situ treatment, which includes full dynamics for five species: a heavy metal to be remediated, an electron donor, biomass, a nontoxic conservative bio-inhibitor, and a biocide. Direct abiotic reduction by donor-metal interaction as well as donor-driven biomass growth and bio-reduction are modeled, along with crucial processes such as donor sorption, bio-fouling and biomass death. Our software implementation handles heterogeneous flow fields, arbitrarily many chemical species and amendment injection points, and features full coupling between flow and reactive transport. We describe installation and usage and present two example simulations demonstrating its unique capabilities. One simulation suggests an unorthodox approach to remediation of Cr(VI) contamination.

1 Introduction

Heavy metals, including chromium, arsenic, copper, nickel, selenium, technetium, uranium, and zinc, are widespread and hazardous subsurface contaminants in groundwater aquifers (Appelo and Postma, 2004; Tchounwou et al., 2012). For many heavy metals, their most stable oxidation state is often the most toxic (Duruibe et al., 2007; Hashim et al., 2011), and this oxidation state is typically the highest that occurs under near-surface conditions. Additionally, the chemical reduction of certain metals is known to reduce their mobility (Violante et al., 2010). This has inspired efforts to manipulate in situ conditions to stimulate microbial growth and achieve biologically mediated metal reduction. This technique has been demonstrated, at least in some settings, for chromium, uranium and selenium (Lovley, 1993, 1995), nickel (Zhan et al., 2012), technetium (Istok et al., 2004), and copper (Andreazza et al., 2010), and has been noted as a viable bioremediation technique by recent critical reviews (Hashim et al., 2011; Wu et al., 2010). Bioprecipitation, a process by which microbiological exudates react with metals to produce an insoluble compound, has been widely observed (Malik, 2004; Van Roy et al., 2006; Radhika et al., 2006) and has been noted by Wu et al. (2010) as a remediation method. Bio-stimulants have also recently been shown to effectively reduce chromium through abiotic oxidation-reduction (redox) pathways (Chen et al., 2015; Hansen et al., 2016) and, after fermentation, for other metals (Hashim et al., 2011). Naturally, designing a remedial intervention using one of this family of techniques benefits greatly from the use of a multi-dimensional/multi-component numerical model of groundwater flow, contaminant transport, and biogeochemical processes to evaluate different remediation strategies under varying field conditions. The model should be capable of capturing the transport behavior of electron donors, biomass, and other species, dominant biogeochemical reactions, and how these processes influence, and are influenced by, subsurface flow.

Although the development on in situ bioreactive transport models goes back to at least the 1980s, the literature is not vast. Early work focused on in situ bioremediation of toxic organic compounds through oxidation. A thorough mathematical and 2D numerical study representative of this approach is due to Chiang et al. (1991), who presented a three-equation model involving a mobile electron donor (assumed to be the contaminant), mobile dissolved oxygen, and immobile biomass. The contaminant was assumed to be consumed only in the microbial growth reaction, which was linear in biomass, Monod (Monod, 1949) in electron donor, and Monod in electron acceptor. Wheeler et al. (1992) subsequently extended a reactive model of this sort to three dimensions to simulate biodegradation of CH_4. Travis (1993) presented a more complicated, unsaturated three-dimensional model, which introduced Monod dependence on nutrients, and the potential for two electron donors, with one inhibiting the other. This approach was further elaborated upon in a study of TCE degradation (Travis and Rosenberg, 1998) by accounting for living and dead microbes, microbial predators, and first-order kinetic sorption of all aqueous species (microbes were treated as mobile). Another complex oxidation model was developed by Suk et al. (2000), which explicitly modeled both mobile and immobile biomass, contained a decay network, and featured both anaerobic and aerobic oxidation, in competition.

The development of models for metal reduction is comparatively more recent. For U(VI), field-scale modeling studies have been performed on bio-reduction under anaerobic conditions at the Old Rifle Site in Colorado (Li et al., 2010, 2011; Yabusaki et al., 2011). These conceptions treat the contaminant as the sole electron acceptor, with an externally applied electron donor,

and the implied equations have a similar form to those devised by Chiang et al. (1991): linear in biomass, Monod in contaminant, and Monod in electron donor. For clarity, this is expressed symbolically as:

$$\frac{\partial C}{\partial t} \propto \frac{\partial D}{\partial t} \propto B \frac{C}{K_C + C} \frac{D}{K_D + D}, \tag{1}$$

where t is time, C is the heavy metal (U(VI)) concentration, D is the electron donor concentration, B is the biomass concentration, K_C is the metal reduction Monod constant, and K_D is the electron donor Monod constant. K_C and K_D respectively represent the concentration of C and D at which the reaction rate is halved. Recently, Molins et al. (2015) have published a numerical study of a column experiment with multiple species, all of whose dynamics are of the above form, but including an extra chemical inhibition factor. The models of Li et al. (2010, 2011) were implemented at field-scale in CrunchFlow (Steefel et al., 2015), using its capability to represent single and multiple Monod formulations.

Systems of governing reactive transport equations for enzymatic microbial Cr(VI) reduction have been presented by Alam (2004), and by Shashidhar et al. (2007). Shashidhar et al. (2007) described the Cr(VI) degradation reaction slightly differently from Li et al. (2011):

$$\frac{\partial C}{\partial t} \propto \frac{\partial D}{\partial t} \propto B \frac{K_{C'}}{K_{C'} + C} \frac{D}{K_D + D}. \tag{2}$$

$K_{C'}$ is the concentration of Cr(VI) at which the reaction rate is halved, which is similar to K_C. However, although (2) appears superficially similar to (1), the C factor represents entirely different behavior: not as an energy source but rather as an inhibitor. Interestingly, since the RHS of (2) is a proxy for the biomass growth reaction, C consumption is modeled as proportional to biomass growth, but the biomass growth rate is modeled as independent of C. Biomass dynamics are governed by a growth term proportional to donor consumption and a first-order decay term, accounting for eventual biomass die-off. Other authors (e.g., Somasundaram et al., 2009) have used a similar approach. Alam (2004) presented a relatively complex model which included transport with both mobile and immobile biomass, and also included two enzymes (both created due to biomass growth, but one conserved, and one irreversibly consumed during bio-reduction). Neglecting the irreversibly-consumed enzyme and the mobile-immobile behavior, this model shares its electron donor and biomass dynamics with the model of Shashidhar et al. (2007). It differs significantly from other models that we are aware of by treating the Cr(VI) degradation reaction in this model as an incidental enzymatic process, and is governed by the following Monod equation:

$$\frac{\partial C}{\partial t} \propto B \frac{C}{K_C + C}. \tag{3}$$

There is strong experimental support for this approach (e.g., Okeke, 2008), and this is arguably more defensible in a real, complex geochemical system in which there are multiple competing donors and receptors, and given that there is evidence for indirect reduction pathways, e.g., by metabolites (Priester et al., 2006). All of the models of Cr(VI) bio-reduction discussed above appear to be one-dimensional only.

A general three-dimensional bio-reactive transport model (not specifically focused on heavy metals) which models biomass as a separate species, and explicitly models electron donors and acceptors was presented by Schafer et al. (1998). Biomass growth is taken to be proportional to biomass concentration, with arbitrary user-selectable Monod and inhibition terms, and

biomass decay is taken to be a first-order process with no positive floor value. Unlike the models discussed above, donor and acceptor consumption rates are taken to be proportional to the biomass concentration growth rate, rather than its magnitude. A more recent code, GeoSysBRNS (Centler et al., 2010, 2013), also models general three-dimensional multi-species transport processes with bio-mediated $A + B \rightarrow C$ reactions, but with somewhat simpler biomass dynamics than that presented by Schafer et al. (1998).

Our literature review did not reveal discussion of field-scale bio-reduction models for heavy metal species besides uranium. It thus appears that the primary example of a bio-reduction model applicable to modeling a real-world remediation scheme is the CrunchFlow model of uranium treatment at the Rifle site, which was discussed above. We set out to develop a new model, dubbed CHROTRAN, which is optimized for modeling bioremediation of Cr(VI), but of sufficient generality that it may be used for bioremediation of other metals, or for abiotic reduction, with ease. The key features of the model we developed are as follow:

Direct abiotic reaction between electron donor and contaminant Recent experimental results (Chen et al., 2015; Hansen et al., 2016) have established a rapid direct redox reaction when molasses is used as an electron donor and Cr(VI) is the contaminant, rather than the bio-mediated reaction previously posited. It is thus crucial to include this behavior in a model aimed at remediation design.

Indirect Monod kinetics On account of the evidence (Wang and Xiao, 1995; Okeke, 2008; Hansen et al., 2016) for modeling Cr(VI) degradation with (3), we implemented this general formulation as opposed to one which ties all contaminant degradation to a single biomass growth equation.

Bio-fouling / Bio-clogging It is well known in practice that one of the problems afflicting bioremediation schemes is build-up of biological material near the amendment injection point. This reduces the hydraulic conductivity, interfering with amendment injection, and may rapidly consume any amendment that does manage to pass through it. The model thus contains feedback between local biomass concentration and flow parameters such as porosity and hydraulic conductivity.

Biomass crowding Similarly, if biomass becomes overly dense, this causes cell stress, which reduces the rate of further growth. Since clogging is enabled, this behavior was added as well.

Modeling of amendment additives To address clogging or to attempt to spread electron donors farther from the well before they are consumed, additional chemicals may be injected to reduce biomass concentrations, and their reactive transport behavior is incorporated.

Multiple donor consumption pathways The best model of electron donor consumption by biomass may be proportional to biomass concentration or biomass growth, and the model can handle any such combination.

Building this functionality required custom programming beyond what is embedded in existing reactive transport codes (Steefel et al., 2015). To accomplish our goal, we turned to PFLOTRAN (Lichtner et al., 2017a, b), which is open source and has a modular structure featuring a "reaction sandbox" interface (Hammond, 2015) that allows derivative versions with custom

reaction behavior to be developed and compiled. We developed CHROTRAN based on the existing PFLOTRAN code, taking advantage of the reaction sandbox interface to implement complex model features not included in its basic microbial packages while leveraging other aspects of PFLOTRAN, such as its high-performance computing capabilities. No changes to the flow and transport part of PFLOTRAN were needed.

In Section 2, we present the mathematical details of CHROTRAN and justify some of the decisions underlying the model. In Section 3, we present two numerical studies which illustrate CHROTRAN and also suggest an interesting conclusion regarding Cr(VI) remediation. In Section 4, we briefly summarize what has been presented. The CHROTRAN 1.0 user manual is presented in Appendix A, which gives instructions on how to install and use the software.

2 Model description

We consider flow and transport at aquifer scale. Conceptually, the aquifer is modeled as saturated, with incompressible water moving in accordance with Darcy's law. We note that, since CHROTRAN is built on top of PFLOTRAN, it inherits all of PFLOTRAN's groundwater flow modeling capabilities. This includes the ability to consider unsaturated and otherwise multiphase flow conditions, which are out-of-scope for the present discussion. Please see the PFLOTRAN user manual (Lichtner et al., 2017a) for details on its complete capabilities. Two transport processes are considered, namely, advection with Darcy flow and Fickian dispersion. Multiple reaction terms are then added in order to capture the complex chemical dynamics during remediation. As the model is intended to be used for remedial design, every effort was made to simplify the formulation to use the smallest number of explanatory variables and parameters, and to keep the equations at a high level of abstraction, so they are not tied to one particular set of chemical species.

The following are the several species whose dynamics are captured by the system of reaction equations, each with their own symbols:

Biomass, $B\,[\mathrm{mol\,m_b^{-3}}]$**,** representing the concentration of all microbes and their associated extracellular material. The concentration of biomass is expressed in terms of bulk volume ($\mathrm{m_b^3}$), which includes both the volume of the porous medium and the solution. The quantification of biomass as a "molar" rather than a mass concentration is unusual, and was done for two reasons: (i) to avoid hard-coding units in which biomass concentration is to be specified, and (ii) to simplify presentation of the model, so all governing equations have the same units. A mole of biomass should be understood as an equivalent mass: any quantity can be used, as long as one uses a consistent definition throughout the model. In the examples in this paper, we use the definition 1 mol $\equiv$ 1 g of biomass.

Aqueous contaminant, $C\,[\mathrm{mol\,L^{-1}}]$**,** which we here assume is a heavy metal ion in its oxidized state, such as Cr(VI) or U(VI).

Electron donor, which is part of the chemical amendment, and may be

1. immobile, represented by $D_i\,[\mathrm{mol\,m_b^{-3}}]$, or

2. mobile, represented by D_m [mol L^{-1}],

with exchange of mass between the two states.

Nonlethal biomass-growth inhibitor, I [mol L^{-1}]**,** such as ethanol, which is modeled as a conservative species but acts to slow microbial growth.

Biocide, X [mol L^{-1}]**,** which reacts directly with biomass and is consumed.

For convenience, we also define a total species aqueous concentration of the electron donor, D, according to the formula $D = \frac{D_i}{\theta(\boldsymbol{x},t)10^3} + D_m$ [mol L^{-1}], where $\theta(\boldsymbol{x},t)$ [-] is the current porosity at $\boldsymbol{x}$. For simplicity, we assume that both the mobile and immobile donor participate equally in all reactions. In reality, of course, bio-availability may differ between mobile and immobile species. However, as long as the two phases are near equilibrium, we may calibrate effective reaction rates that ostensibly utilize both phases equally. This is what we have done.

2.1 Flow and transport

2.1.1 Groundwater flow equations

Flow may be modeled using the balance of water mass given by

$$\frac{d}{dt}(\rho_w\theta) + \nabla\cdot\boldsymbol{q} = q_M(\boldsymbol{x},t), \tag{4}$$

with the water mass fluxes related to head via Darcy flux $\boldsymbol{q}$:

$$\boldsymbol{q} = -\nabla\left(\rho_w K(\boldsymbol{x},\boldsymbol{t})h(\boldsymbol{x},t)\right), \tag{5}$$

where ρ_w [kg m^{-3}] is the density of water, $q_M(\boldsymbol{x})$ [kg m^{-3} s^{-1}] is the local mass injection rate into the system, $K(\boldsymbol{x})$ [m s^{-1}] is the local hydraulic conductivity, and $h(\boldsymbol{x},t)$ [m] is the local hydraulic head.

The hydraulic conductivity is continually updated in accord with the relation

$$K(\boldsymbol{x},t) = K(\boldsymbol{x},0)\frac{\theta(\boldsymbol{x},t)}{\theta_0}, \tag{6}$$

where θ_0 [-] is the spatially-uniform initial porosity, and $\theta(\boldsymbol{x},t)$ is calculated according to

$$\theta(\boldsymbol{x},t) = \theta_0 - \frac{B(\boldsymbol{x},t)}{\rho_B}, \tag{7}$$

where ρ_B [mol L^{-1}] is the intrinsic biomass density. (Note that, using our proposed definition of 1 mol of biomass as 1 g of biomass, 1 mol L^{-1} = 1 kg m^{-3}.)

2.1.2 Advective-dispersive transport operator

We define $\mathscr{T}\{\cdot\}$ to be an advective-dispersive transport operator, which characterizes the hydrodynamic effects on solute transport. For c, the concentration of an arbitrary mobile species,

$$\mathscr{T}\{c\} \equiv -\boldsymbol{q}\cdot\nabla c + \nabla\cdot(\theta \boldsymbol{D}(\boldsymbol{q})\nabla c), \tag{8}$$

where $\boldsymbol{D}$ is a dispersion tensor that depends on the longitudinal and transverse dispersivities, molecular diffusion as well as the Darcy flux. For the work in this paper, we will only consider isotropic diffusion, and thereby we set $\boldsymbol{D} = D_m \boldsymbol{I}$, although CHROTRAN can handle more general dispersion tensors. Note that, while this is not shown explicitly for compactness, all symbols in (8) are functions of $\boldsymbol{x}$ and t.

2.2 Biogeochemical reactions

We define one governing equation for each species, mobile or immobile, as well as two equations defining reaction rate expressions for algebraic convenience. The governing equations include kinetically-limited redox reactions. These reactions are often non-instantaneous with redox-sensitive species remaining in thermodynamic disequilibrium (Keating and Bahr, 1998), and a kinetic formulation is a fair representation of this type of behavior (Steefel and MacQuarrie, 1996). The equations involve numerous parameters, whose symbols, units, and long-form name in the CHROTRAN input file are summarized in Table 2. The parameter symbols follow a scheme in which the first letter encodes the physical interpretation of the parameter and the subscript specifies the governing equation in which they participate. A symbol beginning with Γ is a second-order mass action rate constant, with units [L mol^{-1} s]. A symbol beginning with K is Monod or inhibition constant with units of concentration, mol m_b^{-3} or mol L^{-1}, and represents the concentration at which a process rate becomes 50% of its maximum rate, all other parameters being equal. A symbol beginning with λ has units of s^{-1} and is interpreted as a pure first-order reaction rate constant. A symbol beginning with S is dimensionless, and represents a stoichiometric relationship between a reaction rate and the consumption rate of a certain species.

Before presenting the equations, it is useful to review all of the biochemical processes that are incorporated into the model:

Abiotic reduction This is an aqueous-phase bimolecular reaction between the electron donor, D, and the contaminant, C. It is modeled with a classical second-order mass action rate law.

Bio-reduction This represents the removal of the contaminant, C by the biomass, B. The process is assumed to be linear in B and Monod in C. Note that we are not assuming that reduction of C is directly tied to any particular cell metabolic process. This form is sufficiently general that it can capture other bio-remediation processes besides bio-reduction of heavy metals.

Biocide reaction This is an inter-phase bimolecular reaction between the biocide, X, and the biomass, B. It is modeled with a classical second-order mass action rate law, with the added condition that B cannot fall below a specified minimum concentration $B_{\min}$.

Biomass growth The core biomass growth reaction irreversibly consumes electron donor, D, to increase biomass, B. As a biologically catalyzed reaction, it is assumed to be linear in B and Monod in C. Two inhibition effects are assumed: a biomass crowding term, tunable with exponent α, attenuates growth rate as the biomass concentration rises. The nonlethal inhibitor concentration, I, also reduces the reaction rate as its concentration increases.

Mobile-immobile mass transfer (MIMT) This is a process with first-order kinetics, which models sorptive retardation of the electron donor.

Natural decay This is an empirical process reflecting the idea that, if left unstimulated, both the amount of living cells and the amount of extracellular material in the aquifer will ultimately return to their natural background level (i.e. $B_{\min}$). This is modeled as a first-order process. Our model assumes that reduction is occurring as a dissimilatory reaction that occurs extracellularly, so biomass decay does not directly release heavy metal.

Respiration This represents consumption of the electron donor for purposes of life maintenance, unrelated to biomass growth. This is described by a first-order rate law which is proportional to biomass concentration, B.

The explanations of the operative processes and of parameter interpretation above help the descriptions of factors and terms in the governing equations presented below.

2.3 Reactive transport equations

2.3.1 Definitions of convenience reaction variables

The biomass growth reaction is linear in biomass concentration, has a Monod dependency on electron donor, a tunable inhibition factor due to biomass crowding, and a classic inhibition factor describing the impact of the nonlethal growth inhibitor (as indicated by comment braces):

$$\mu_B = \lambda_{B_1} B \overbrace{\frac{D}{K_D + D}}^{e^- \text{donor}} \underbrace{\left(\frac{K_B}{K_B + B}\right)^{\alpha}}_{\text{crowding}} \overbrace{\frac{K_I}{K_I + I}}^{\text{inhibition}} \qquad \left[\frac{\text{mol}}{\text{m}_\text{b}^3\,\text{s}}\right]. \tag{9}$$

The direct, abiotic reduction reaction is represented by a classical second-order mass action law:

$$\mu_{CD} = \Gamma_{CD} C D \qquad \left[\frac{\text{mol}}{\text{L s}}\right]. \tag{10}$$

2.3.2 Partial differential equations for mobile chemical components

The mobile components are all governed by the advection-dispersion operator, $\mathscr{T}$, defined previously, and also affected by extra terms implementing the chemical processes outlined earlier (as indicated by comment braces):

$$\frac{\partial \theta C}{\partial t} = \mathscr{T}\{C\} - \overbrace{\lambda_C B \frac{C}{K_C + C}}^{\text{bio-reduction}} - \underbrace{S_C \mu_{CD}}_{\text{abiotic reduction}} \qquad \left[\frac{\text{mol}}{\text{m}_\text{b}^3\,\text{s}}\right], \tag{11}$$

$$\frac{\partial \theta D_m}{\partial t} = \mathscr{T}\{D_m\} - \overbrace{S_{D_1} \frac{D_m}{D} \mu_B}^{\text{biomass growth}} - \underbrace{\lambda_D \frac{D_m}{D} B}_{\text{respiration}} - \overbrace{S_{D_2} \theta \mu_{CD} \frac{D_m}{D}}^{\text{abiotic reduction}} - \underbrace{\lambda_{D_i} \theta D_m + \lambda_{D_m} D_i}_{\text{MIMT}} \qquad \left[\frac{\text{mol}}{\text{m}_\text{b}^3\,\text{s}}\right], \tag{12}$$

$$\frac{\partial \theta I}{\partial t} = \mathscr{T}\{I\} \qquad \left[\frac{\text{mol}}{\text{m}_\text{b}^3\,\text{s}}\right], \tag{13}$$

$$\frac{\partial \theta X}{\partial t} = \mathscr{T}\{X\} - \overbrace{\Gamma_X B X}^{\text{biocide reaction}} \qquad \left[\frac{\text{mol}}{\text{m}_\text{b}^3\,\text{s}}\right]. \tag{14}$$

2.3.3 Partial differential equations for immobile chemical components

The immobile component concentrations are affected only by the reactive processes outlined above (again, indicated by comment braces):

$$\frac{\partial B}{\partial t} = \overbrace{\mu_B}^{\text{biomass growth}} - \underbrace{\lambda_{B_2}(B - B_{\min})}_{\text{natural decay}} - \overbrace{\Gamma_B (B - B_{\min}) X}^{\text{biocide reaction}} \qquad \left[\frac{\text{mol}}{\text{m}_\text{b}^3\,\text{s}}\right], \tag{15}$$

$$\frac{\partial D_i}{\partial t} = -\overbrace{S_{D_1} \frac{D_i}{D} \mu_B}^{\text{biomass growth}} - \underbrace{\lambda_D \frac{D_i}{D} B}_{\text{respiration}} - \overbrace{S_{D_2} \theta \mu_{CD} \frac{D_i}{D}}^{\text{abiotic reduction}} + \underbrace{\lambda_{D_i} \theta D_m - \lambda_{D_m} D_i}_{\text{MIMT}} \qquad \left[\frac{\text{mol}}{\text{m}_\text{b}^3\,\text{s}}\right]. \tag{16}$$

3 CHROTRAN validation and remediation case studies

The PFLOTRAN software from which CHROTRAN derives its numerical flow and reactive transport solvers has gone through extensive quality assurance testing (Hammond et al., 2014; Hammond and Frederick, 2016; Hammond, 2017), has been benchmarked against other reactive transport solvers (Lichtner et al., 2017a), and is used inside and outside the U.S. Department of Energy for mission-critical analytical work (e.g. Hammond et al., 2012; Navarre-Sitchler et al., 2013; Karra et al., 2014; Zachara et al., 2016). The new bio-reactive transport model that is constitutive of CHROTRAN is not available in any other software, so direct benchmarking is not possible. However, extensive quality testing has been performed by the developers. We have validated the code through batch and multi-dimensional simulations that CHROTRAN does satisfy the governing equations we present for chemistry and permeability, and also that it gives plausible, physically consistent results for a wide range of scenarios. In particular, the repository includes batch regression tests cover abiotic reaction, abiotic reaction with sorption (MIMT), microbial growth and decay, as well as interaction with biocide and nonlethal inhibitor. In addition, a non-batch reference simulation featuring bio-clogging is included. These benchmarks are located in subdirectories of the `chrotran_benchmarks` directory in the developer branch (`dev`) of the CHROTRAN repository. In the top-level directory resides a bash script, `chrotran_benchmarks.sh` that runs all the regression tests.

To demonstrate the novel capabilities of our software, we present two example studies, which together illustrate the interactions of all the types of chemical species it permits to be modeled, along with its treatment of bio-clogging. The input and auxiliary files for these two examples can be found in the `chrotran_examples` directory in the CHROTRAN repository.

3.1 Case study: remediation of Cr(VI) by molasses and ethanol co-injection

This study concerns the co-injection of molasses (electron donor, D) and ethanol (nonlethal bio-inhibitor, I) into a single well drilled in a heterogeneous aquifer with an appreciable background Cr(VI) concentration. The competition between direct abiotic reduction of Cr(VI) by molasses and bio-reduction of Cr(VI), which exists since both reduction pathways consume the electron donor, along with the impact of suppressing the biomass growth is explored. The basic parameters used are those shown in Figures A1 and A2, with changes as indicated below.

Four related simulations are performed on the same 100×100 m^2 two-dimensional heterogeneous hydraulic conductivity field, with geometric mean conductivity $K_g = 10^{-4}$ m s^{-1}, a multi-Gaussian correlation structure with exponential semivariogram with correlation length of 4 m and $\sigma^2_{\ln K} = 2$. Each simulation takes place over a span of 500 days and begins with $\varepsilon = 10^{-20}$ mol L^{-1} initial concentrations of all species, except $C = 1.923 \times 10^{-5}$ mol L^{-1} (1000 ppb Cr(VI)), $B = B_{min} = 10^{-10}$ mol m$_b^{-3}$ and $D_i = 10^{-20}$ mol m$_b^{-3}$. In all cases, there are no flow boundaries at the north and south of the domain ($y = 0$ m and $y = 100$ m), and constant head boundaries are imposed at the west and east of the domain ($x = 0$ m and $x = 100$ m) such that there is a drop of head of 0.28 m between these faces. A single injection well exists at $(x, y) = (25\text{ m}, 50\text{ m})$. For the first 10 days of the simulation, there is no injection into the well. From 10 d to 30 d, injection is performed at the well with

constant volumetric flow rate 272.55 $m^3 d^{-1}$ with species concentrations discussed below. From 30 d to 500 d, there is again no injection at the well. A very large (arbitrary) ρ_B is assumed, so as to eliminate the effect of biomass clogging from this simulation.

The four simulations differ in their chemistry only. Two direct abiotic reduction rates are considered: $\Gamma_{CD} = 1$ L mol^{-1} s^{-1} and $\Gamma_{CD} = 0$ L mol^{-1} s^{-1}, as are two different ethanol concentrations in the injection fluid: $I = 1$ mol L^{-1} and $I = \varepsilon$ mol L^{-1}, in all four possible combinations. The injection fluid chemistry always has Cr(VI) concentration equal to the initial concentration ($C = 1.923 \times 10^{-5}$ mol L^{-1}), ensuring that no chromium disappearance is due to dilution, and molasses concentration $D = 1 \times 10^{-2}$ mol L^{-1}.

Concentrations of Cr(VI) for each scenario are shown in Figure 1. It is apparent that little persistent reduction due to biomass alone occurs, although ethanol co-injection does increase biomass footprint, which has a noticeable and persistent effect. By contrast, the rapid abiotic reaction between Cr(VI) and a constituent of molasses has more impact. This is attributable to the fact that molasses has a large reducing capacity, background concentrations of Cr(VI) are relatively low, and it has a retardation factor of around 150 (obtained from Shashidhar et al. (2006)), meaning that it has the potential to form a persistent permeable reactive barrier around the well. The better performance in the presence of ethanol is attributable to the fact that ethanol co-injection prevented consumption of molasses by the biomass during the injection phase, and so molasses persists over a larger area.

3.2 Case study: biomass clogging/unclogging due to acetate/dithionite injection

CHROTRAN has the capability to model hydraulic conductivity reduction due to bio-fouling and the use of biocide as a remediation strategy. To illustrate model capabilities, we perform a simulation of constant-head injection into a homogeneous aquifer in which the injection fluid is amended initially with the biostimulant acetate ($D = 10^{-2}$ mol L^{-1}) for the first 400 d. The acetate amendment is subsequently replaced with the biocide dithionite ($X = 3.5$ mol L^{-1}), for the remainder of the simulation. The basic structure of the CHROTRAN input file is the same as in the study outlined in Section 3.1 (this is to say, as shown in Figures A1 and A2), but with different CHROTRAN parameter values, as shown in Table 1. We here make the reasonable (Ritmann, 2004, p. 361) assumption that biomass has the same density as water (recall that we everywhere use the interpretation that 1 mol of biomass is defined as 1 g of biomass).

The simulation is performed on a 50 m square homogeneous hydraulic conductivity field, with constant hydraulic conductivity $K = 9.8 \times 10^{-5}$ m s^{-1} and initial porosity $\theta = 0.15$. Each simulation takes place over a span of 500 days, and begins with $\varepsilon = 10^{-20}$ mol L^{-1} initial concentrations of all species, except $C = 1.923 \times 10^{-5}$ mol L^{-1} (1000 ppb Cr(VI)), $B = B_{min} = 10^{-10}$ mol m_b^{-3} and $D_i = 10^{-20}$ mol m_b^{-3}. No flow boundaries are imposed at the north and south of the domain ($y = 0$ m and $y = 50$ m), and constant head boundaries are imposed at the west and east of the domain (head 0.28 m at $x = 0$ m and head 0 m at $x = 50$ m). A single injection well exists at $(x, y) = (25\text{ m}, 25\text{ m})$, and constant head of 0.28 m is imposed at its location.

A sequence of quiver plots representing the velocity field at nine points in time, superimposed on the intensity of biomass concentration are shown in Figure 2. During the first 400 d of the simulation, biomass concentration grows in the vicinity of the well, until hydraulic conductivity drops to zero at the well and no influx occurs there; only ambient flow is apparent, flowing around the impermeable biomass barrier near the well. At this point, the biomass has become useless for bioremediation, as contaminated aquifer water no longer travels through it. However, at 400 d, dithionite is introduced into the injection fluid and effectively eliminates biomass in the vicinity of the well. The region containing dithionite is relatively sterile and grows outwards until the biomass concentration approaches background, and the initial flow regime is recovered at 416 d. Because initial and final conditions are the same, this cycle may be performed indefinitely.

4 Summary and conclusions

For modeling in situ remediation of aqueous groundwater contaminants by injection of aqueous amendment, we recognized the importance of mathematical formulations and numerical codes that can represent multi-dimensional fluid flow and multi-species contaminant transport in heterogeneous aquifers with arbitrary injection regimes. For the particularly important case of heavy metal remediation, a number of contaminant-remediation processes (pathways) are amenable to a unified modeling framework: bio-reduction, bio-precipitation, and direct reduction by the chemical amendment. There have previously existed no general tools appropriate for modeling such interventions. With this background in mind, we developed a mathematical model that describes the reactive transport dynamics of an amendment (containing any combination of electron donor, non-lethal bio-inhibitor, and biocide) with biomass and aqueous heavy metal contaminant. We also implemented the mathematical model in a novel computational framework, called CHROTRAN, that is based on the open-source code PFLOTRAN. PFLOTRAN's modularity and the reaction sandbox capability allowed us to implement the model easily without making any changes to the flow and transport code of PFLOTRAN. CHROTRAN can harness the existing capabilities of PFLOTRAN, which allows for simulations of complex models with a large number of computational cells and degrees of freedom. We described our computer implementation and explained how to use CHROTRAN to solve practical problems.

We also considered two demonstration studies related to chromium remediation. The presented synthetic problems were formulated to be consistent with real-world groundwater contamination problems and illustrate the capability of CHROTRAN to aid in the engineering design process. In one of the studies, we discovered that, contrary to much existing theory, Cr(VI) reduction was maximized by injecting molasses and suppressing biomass growth to maximize the direct, abiotic reduction reaction. In the other, we showed the feasibility of pulsed injection of bio-stimulant and biocide to alleviate bio-fouling in the context of ongoing bioremediation.

We observe that because of the abstraction of our model and its parametric flexibility, the CHROTRAN equations can be used to model other reactive transport behaviors besides the heavy metal bio-reduction that we have focused upon, including basic advection-dispersion-reaction interaction (between C and D, in the absence of B). The bio-reduction model captures any biodegradation that can be represented using a Monod equation, as long as the contaminant represented by C is non-sorbing,

and it does not explicitly require the contaminant to be reduced. This potentially allows for modeling the biodegradation of a wide range of organic contaminants, which include but are not limited to hydrocarbons, chlorinated solvents, pesticides, and volatile organic compounds.

Code availability. The Fortran source code files for CHROTRAN, along with input files for the examples presented in this document, are freely available at https://github.com/chrotran/release, released under the GPL 3 license. Additional information regarding CHROTRAN is available at http://chrotran.lanl.gov.

Appendix A: User manual

A1 Installing CHROTRAN

CHROTRAN must be compiled using the GFortran compiler (freely available as part of the GNU Compiler Collection). It is based on the open-source PFLOTRAN code base, the installation procedure is essentially the same as that required to build PFLOTRAN from source, and CHROTRAN requires all the libraries upon which PFLOTRAN depends, including PETSc (Balay et al., 2016) and others. CHROTRAN 1.0 is based upon PFLOTRAN commit `8f33d80`, which requires PETSc commit `03c0fad` (tag `xsdk-0.2.0`). For installation of required libraries, the PFLOTRAN installation instructions[1] are applicable, except that CHROTRAN, rather than PFLOTRAN, should be cloned from its repository[2] once all the dependencies have installed. To build CHROTRAN itself, navigate to `<path of cloned repository>/src/pflotran` and type `make chrotran`. (The CHROTRAN executable will be called `chrotran`.)

A2 Specifying and running a simulation

A CHROTRAN input file is of the same format as a PFLOTRAN input file. Information on how to set up such a file is available in the PFLOTRAN user manual (Lichtner et al., 2017a). However, to use CHROTRAN's additional functionality, a few of the input cards (top-level blocks, in PFLOTRAN jargon) must contain some particular content. The required `CHEMISTRY` card format is shown in Figure A1, with bold text being mandatory and standard-weight text being user-alterable. The required `SIMULATION`, `MATERIAL_PROPERTY`, and (initial) `CONSTRAINT` card formats are shown in Figure A2, again with bold text being mandatory and standard-weight text being user-alterable. Comments in the input file are preceded by the character `#`.

In addition to these cards being properly formatted, there must exist a chemistry database at the (absolute or relative) path specified after the `DATABASE` keyword in the `CHEMISTRY` card, and it must, at a minimum contain the lines shown in Figure A3. The one exception to bold text being mandatory is that species *names* can be changed at will, as long as there is consistency

[1] Available at http://documentation.pflotran.org/user_guide/how_to/installation/installation.html.
[2] Available at https://github.com/chrotran/release

between the CHEMISTRY card and the chemistry database. For instance, one could change all instances of the text Cr(VI) in both of those locations to U(VI) or all instances of the text chubbite to etibbuhc, with no alteration in execution behavior (besides, obviously, the species names used in the output files).

The chemistry database contains lines for five mobile species: water, plus the mobile species in the CHROTRAN kinetics listed in Section 2.3: C, D_m, I, and X. The database also contains a line for a "dummy" mineral species, chubbite, which does not correspond to any species previously mentioned. This species is treated as a mineral which is specified as inactive with respect precipitation/dissolution by setting its kinetic rate constant (RATE_CONSTANT) to zero. The mineral is included as a surrogate for biomass and porous media volume in CHROTRAN and is updated according to Equation 7 to track $1-\theta(\boldsymbol{x},t)$. The initial volume fraction of chubbite thus defines the initial porosity. The format of a chemistry database is discussed in more detail in the PFLOTRAN user manual.

Once you have saved your input file as, e.g. test.in, it is easy to run the code from the console. Navigate to <path of cloned repository>/src/pflotran, and type chrotran -pflotranin <path to input file>/test.in. The output of the simulation will be saved in the same directory as the input file. Depending on the options specified in the input file, CHROTRAN can save flow field velocities, concentrations of all species, permeabilities, and porosities at any specified times in an .h5 format file. This file format can be visualized natively using freely-available standalone tools such as VisIt (Childs, 2013) and ParaView (Ahrens et al., 2005), and are also accessible from Python scripts by means of the h5py library and from Julia scripts by means of the HDF5 package.

Competing interests. The authors declare no competing interests.

Acknowledgements. The authors acknowledge the support of the Los Alamos National Laboratory Environmental Programs.

References

Ahrens, J., Geveci, B., and Law, C.: Paraview: An end-user tool for large data visualization, The Visualization Handbook, 717, 2005.

Alam, M.: Bioreduction of hexavalent chromium: flow-through column experiments and reactive transport modeling, Ph.D. thesis, Washington State University, 2004.

Andreazza, R., Pieniz, S., Wolf, L., Lee, M. K., Camargo, F. A. O., and Okeke, B. C.: Characterization of copper bioreduction and biosorption by a highly copper resistant bacterium isolated from copper-contaminated vineyard soil, Science of the Total Environment, 408, 1501–1507, doi:10.1016/j.scitotenv.2009.12.017, http://dx.doi.org/10.1016/j.scitotenv.2009.12.017, 2010.

Appelo, C. A. J. and Postma, D.: Geochemistry, groundwater and pollution, CRC press, 2004.

Balay, S., Abhyankar, S., Adams, M., Brown, J., Brune, P., Buschelman, K., Dalcin, L., Eijkhout, V., Gropp, W., Karpeyev, D., Kaushik, D., Knepley, M., Curfman McInnes, L., Rupp, K., Smith, B., Zampini, S., Zhang, H., and Zhang, H.: PETSc Users Manual, Tech. Rep. ANL-95/11 Rev 3.7, Argonne National Laboratory, 2016.

Centler, F., Shao, H., De Biase, C., Park, C. H., Regnier, P., Kolditz, O., and Thullner, M.: GeoSysBRNS-A flexible multidimensional reactive transport model for simulating biogeochemical subsurface processes, Computers and Geosciences, 36, 397–405, doi:10.1016/j.cageo.2009.06.009, http://dx.doi.org/10.1016/j.cageo.2009.06.009, 2010.

Centler, F., Heß e, F., and Thullner, M.: Estimating pathway-specific contributions to biodegradation in aquifers based on dual isotope analysis: Theoretical analysis and reactive transport simulations, Journal of Contaminant Hydrology, 152, 97–116, doi:10.1016/j.jconhyd.2013.06.009, http://dx.doi.org/10.1016/j.jconhyd.2013.06.009, 2013.

Chen, Z.-F., Zhao, Y.-S., Zhang, J.-W., and Bai, J.: Mechanism and Kinetics of Hexavalent Chromium Chemical Reduction with Sugarcane Molasses, Water, Air, & Soil Pollution, 226, 1–9, doi:10.1007/s11270-015-2629-6, 2015.

Chiang, C. Y., Dawson, C. N., and Wheeler, M. F.: Modeling of in-situ biorestoration of organic compounds in groundwater, Transport in Porous Media, 6, 667–702, doi:10.1007/BF00137855, 1991.

Childs, H.: VisIt: An end-user tool for visualizing and analyzing very large data, LBNL-6320E, Lawrence Berkeley National Laboratory, 2013.

Duruibe, J. O., Ogwuegbu, M. O. C., Egwurugwu, J. N., and Others: Heavy metal pollution and human biotoxic effects, International Journal of Physical Sciences, 2, 112–118, 2007.

Hammond, G. and Frederick, J.: PFLOTRAN Verification: Development of a Testing Suite to Ensure Software Quality, in: 2016 AGU Fall Meeting, 2016.

Hammond, G., Lichtner, P., Lu, C., and Mills, R.: Pflotran: reactive flow & transport code for use on laptops to leadership-class supercomputers, Groundwater reactive transport models, pp. 141–159, 2012.

Hammond, G. E.: PFLOTRAN: Recent Developments Facilitating Massively-Parallel Reactive Biogeochemical Transport, in: 2015 AGU Fall Meeting, American Geophysical Union Fall Meeting, 2015.

Hammond, G. E.: PFLOTRAN Testing, SAND2017-5260PE, Sandia National Laboratories, http://www.osti.gov/scitech/servlets/purl/1367248, 2017.

Hammond, G. E., Lichtner, P. C., and Mills, R.: Evaluating the performance of parallel subsurface simulators: An illustrative example with PFLOTRAN, Water resources research, 50, 208–228, 2014.

Hansen, S. K., Boukhalfa, H., Karra, S., Wang, D., and Vesselinov, V. V.: Chromium (VI) reduction in acetate- and molasses-amended natural media: experimental results and model development, Tech. Rep. LA-UR-16-27473, Los Alamos National Laboratory, 2016.

Hashim, M. A., Mukhopadhyay, S., Sahu, J. N., and Sengupta, B.: Remediation technologies for heavy metal contaminated groundwater, Journal of Environmental Management, 92, 2355–2388, doi:10.1016/j.jenvman.2011.06.009, http://dx.doi.org/10.1016/j.jenvman.2011.06.009, 2011.

Istok, J. D., Senko, J. M., Krumholz, L. R., Watson, D., Bogle, M. A., Peacock, A., Chang, Y. J., and White, D. C.: In Situ Bioreduction of Technetium and Uranium in a Nitrate-Contaminated Aquifer, Environmental Science and Technology, 38, 468–475, doi:10.1021/es034639p, 2004.

Karra, S., Painter, S., and Lichtner, P.: Three-phase numerical model for subsurface hydrology in permafrost-affected regions (PFLOTRAN-ICE v1. 0), The Cryosphere, 8, 1935–1950, 2014.

Keating, E. H. and Bahr, J. M.: Reactive transport modeling of redox geochemistry: Approaches to chemical disequilibrium and reaction rate estimation at a site in northern Wisconsin, Water Resources Research, 34, 3573–3584, 1998.

Li, L., Steefel, C. I., Kowalsky, M. B., Englert, A., and Hubbard, S. S.: Effects of physical and geochemical heterogeneities on mineral transformation and biomass accumulation during biostimulation experiments at Rifle, Colorado, Journal of Contaminant Hydrology, 112, 45–63, doi:10.1016/j.jconhyd.2009.10.006, 2010.

Li, L., Gawande, N., Kowalsky, M. B., Steefel, C. I., and Hubbard, S. S.: Physicochemical heterogeneity controls on uranium bioreduction rates at the field scale., Environmental Science & Technology, 45, 9959–66, doi:10.1021/es201111y, 2011.

Lichtner, P. C., Hammond, G. E., Lu, C., Karra, S., Bisht, G., Andre, B., Mills, R. T., Kumar, J., and Frederick, J. M.: PFLOTRAN User Manual, http://www.documentation.pflotran.org, 2017a.

Lichtner, P. C., Hammond, G. E., Lu, C., Karra, S., Bisht, G., Andre, B., Mills, R. T., Kumar, J., and Frederick, J. M.: PFLOTRAN Web page, http://www.pflotran.org, 2017b.

Lovley, D. R.: Dissimilatory metal reduction, Annual Reviews in Microbiology, 47, 263–290, 1993.

Lovley, D. R.: Bioremediation of organic and metal contaminants with dissimilatory metal reduction., Journal of industrial microbiology, 14, 85–93, doi:10.1007/BF01569889, 1995.

Malik, A.: Metal bioremediation through growing cells, Environment international, 30, 261–278, 2004.

Molins, S., Greskowiak, J., Wanner, C., and Mayer, K. U.: A benchmark for microbially mediated chromium reduction under denitrifying conditions in a biostimulation column experiment, Computational Geosciences, 19, 479–496, doi:10.1007/s10596-014-9432-0, 2015.

Monod, J.: The growth of bacterial cultures, Annual Reviews in Microbiology, 3, 371–394, 1949.

Navarre-Sitchler, A. K., Maxwell, R. M., Siirila, E. R., Hammond, G. E., and Lichtner, P. C.: Elucidating geochemical response of shallow heterogeneous aquifers to CO_2 leakage using high-performance computing: implications for monitoring of CO_2 sequestration, Advances in Water Resources, 53, 45–55, 2013.

Okeke, B. C.: Bioremoval of hexavalent chromium from water by a salt tolerant bacterium, Exiguobacterium sp. GS1, Journal of Industrial Microbiology and Biotechnology, 35, 1571–1579, doi:10.1007/s10295-008-0399-5, 2008.

Priester, J. H., Olson, S. G., Webb, S. M., Neu, M. P., Hersman, L. E., and Holden, P. A.: Enhanced Exopolymer Production and Chromium Stabilization in Pseudomonas putida Unsaturated Biofilms, Applied and Environmental Microbiology, 72, 1988–1996, 2006.

Radhika, V., Subramanian, S., and Natarajan, K. A.: Bioremediation of zinc using Desulfotomaculum nigrificans: Bioprecipitation and characterization studies, Water Research, 40, 3628–3636, doi:10.1016/j.watres.2006.06.013, 2006.

Ritmann, B. E.: Biofilms in the Water Industry, in: Microbial Biofilms, edited by Ghannoum, M. and O'Toole, G., ASM Press, Washington, DC, 2004.

Schafer, D., Schafer, W., and Kinzelbach, W.: Simulation of reactive processes related to biodegradation in aquifers. 1. Structure of the three-dimensional reactive transport model, Journal of Contaminant Hydrology, 31, 187–209, doi:10.1016/S0169-7722(97)00061-2, 1998.

Shashidhar, T., Philip, L., and Bhallamudi, S. M.: Bench-scale column experiments to study the containment of Cr(VI) in confined aquifers by bio-transformation, Journal of Hazardous Materials, 131, 200 – 209, doi:http://dx.doi.org/10.1016/j.jhazmat.2005.09.034, 2006.

Shashidhar, T., Bhallamudi, S. M., and Philip, L.: Development and validation of a model of bio-barriers for remediation of Cr(VI) contaminated aquifers using laboratory column experiments, Journal of Hazardous Materials, 145, 437–452, doi:http://dx.doi.org/10.1016/j.jhazmat.2006.11.034, 2007.

Somasundaram, V., Philip, L., and Bhallamudi, S. M.: Experimental and mathematical modeling studies on Cr(VI) reduction by CRB, SRB and IRB, individually and in combination, Journal of Hazardous Materials, 172, 606–617, doi:10.1016/j.jhazmat.2009.07.043, 2009.

Steefel, C. I. and MacQuarrie, K. T.: Approaches to modeling of reactive transport in porous media, Reviews in Mineralogy and Geochemistry, 34, 85–129, 1996.

Steefel, C. I., Appelo, C. A. J., Arora, B., Jacques, D., Kalbacher, T., Kolditz, O., Lagneau, V., Lichtner, P. C., Mayer, K. U., Meeussen, J. C. L., Molins, S., Moulton, D., Shao, H., Šimůnek, J., Spycher, N., Yabusaki, S. B., and Yeh, G. T.: Reactive transport codes for subsurface environmental simulation, Computational Geosciences, 19, 445–478, doi:10.1007/s10596-014-9443-x, http://dx.doi.org/10.1007/s10596-014-9443-x, 2015.

Suk, H., Lee, K.-K., and Lee, C. H.: Biologically reactive multispecies transport in sanitary landfill, Journal of Environmental Engineering, 126, 419–427, 2000.

Tchounwou, P. B., Yedjou, C. G., Patlolla, A. K., and Sutton, D. J.: Heavy metal toxicity and the environment, in: Molecular, clinical and environmental toxicology, pp. 133–164, Springer, 2012.

Travis, B. J.: Numerical simulation of in situ bioremediation, in: Transactions on Ecology and the Environment, vol. 17, doi:10.2495/AIR990911, 1993.

Travis, B. J. and Rosenberg, N. D.: Modeling in situ bioremediation of TCE at Savannah River: Effects of product toxicity and microbial interactions on TCE degradation, Environmental Science and Technology, 31, 3093–3102, doi:10.1021/es9610186, 1998.

Van Roy, S., Vanbroekhoven, K., Dejonghe, W., and Diels, L.: Immobilization of heavy metals in the saturated zone by sorption and in situ bioprecipitation processes, Hydrometallurgy, 83, 195–203, 2006.

Violante, A., Cozzolino, V., Perelomov, L., Caporale, A. G., and Pigna, M.: Mobility and bioavailability of heavy metals and metalloids in soil environments, Journal of soil science and plant nutrition, 10, 268–292, 2010.

Wang, Y.-T. and Xiao, C.: Factors affecting hexavalent chromium reduction in pure cultures of bacteria, Water Research, 29, 2467–2474, 1995.

Wheeler, M. F., Roberson, K. R., and Chilakapati, A.: Three-Dimensional Bioremediation Modeling in Heterogeneous Porous Media, in: University of Colorado 9th International Conference on Computational Methods in Water Resources, pp. 1–19, Denver, CO, 1992.

Wu, G., Kang, H., Zhang, X., Shao, H., Chu, L., and Ruan, C.: A critical review on the bio-removal of hazardous heavy metals from contaminated soils: Issues, progress, eco-environmental concerns and opportunities, Journal of Hazardous Materials, 174, 1–8, doi:10.1016/j.jhazmat.2009.09.113, 2010.

Yabusaki, S. B., Fang, Y., Williams, K. H., Murray, C. J., Ward, A. L., Dayvault, R. D., Waichler, S. R., Newcomer, D. R., Spane, F. A., and Long, P. E.: Variably saturated flow and multicomponent biogeochemical reactive transport modeling of a uranium bioremediation field experiment, Journal of Contaminant Hydrology, 126, 271 – 290, doi:http://dx.doi.org/10.1016/j.jconhyd.2011.09.002, 2011.

Zachara, J. M., Chen, X., Murray, C., and Hammond, G.: River stage influences on uranium transport in a hydrologically dynamic groundwater-surface water transition zone, Water Resources Research, 52, 1568–1590, 2016.

Zhan, G., Li, D., and Zhang, L.: Aerobic bioreduction of nickel(II) to elemental nickel with concomitant biomineralization, Applied Microbiology and Biotechnology, 96, 273–281, doi:10.1007/s00253-011-3827-9, 2012.

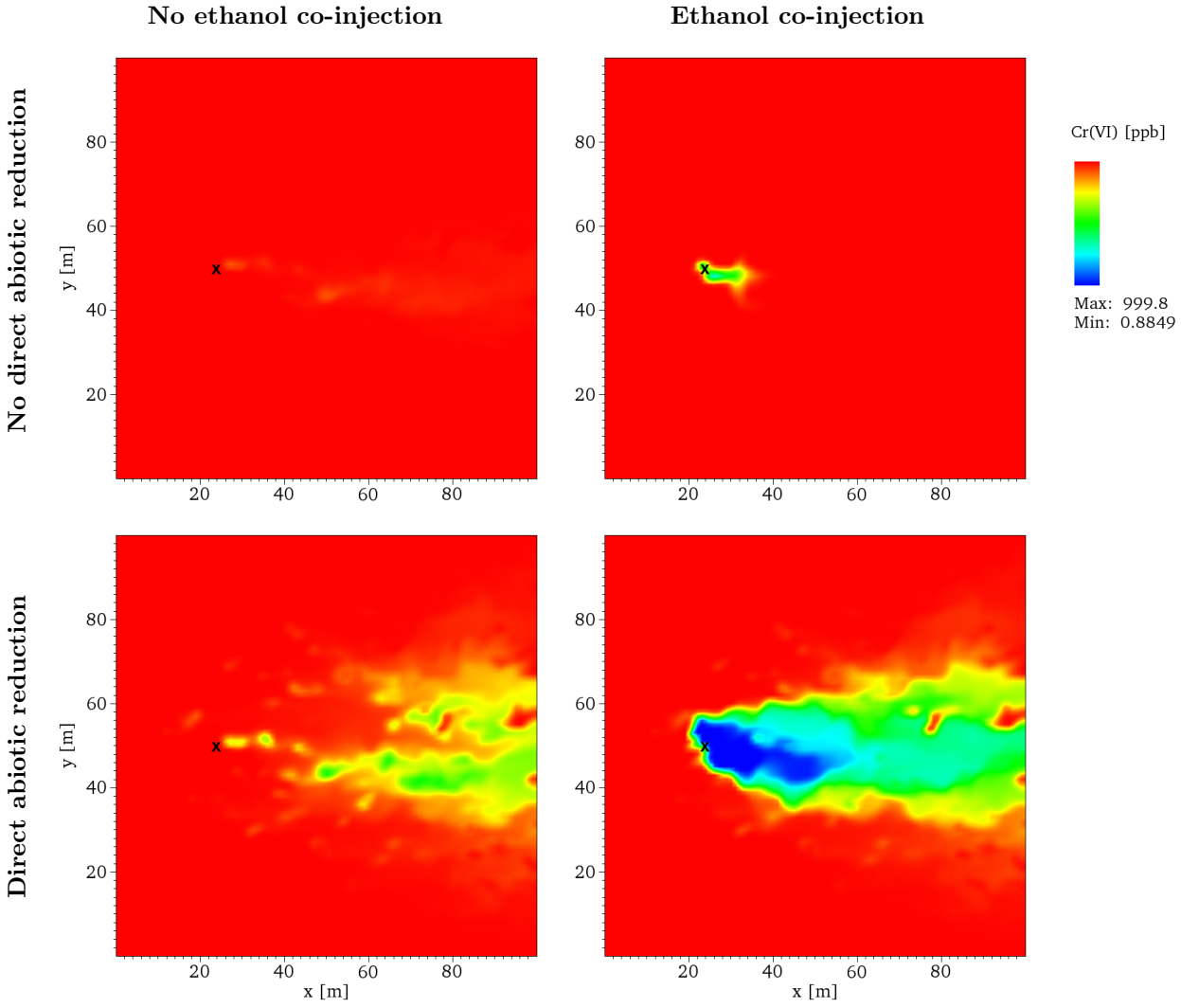

Figure 1. Maps of Cr(VI) concentrations [ppb] in the aquifer 470 d after injection ceased in each of the four scenarios discussed in Section 3.1. Injection well location is denoted by a black *X*.

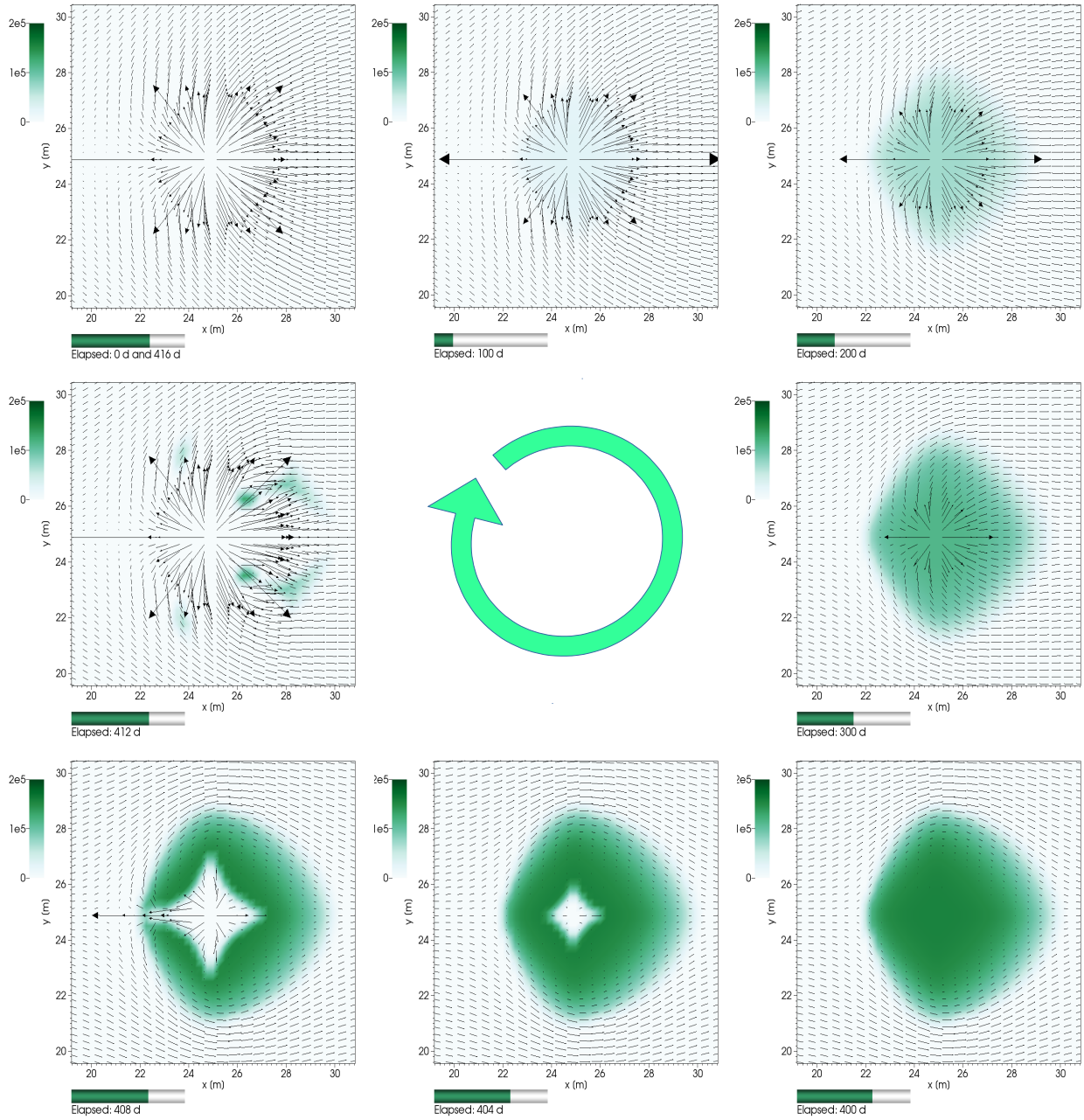

Figure 2. A sequence of snapshots of the cell-center groundwater seepage velocity fields and biomass concentration distributions in the example of Section 3.2. Velocity magnitude is indicated by arrow length and direction by arrow orientation; the arrow tails are located at the cell center; biomass concentration [g m^{-3}] is indicated by green intensity in each superimposed map. The initial condition snapshot is shown in the upper left corner, with time increasing in the clockwise direction, until the initial condition is reached again at 416 d. The same scale is used in each snapshot.

```
CHEMISTRY
  PRIMARY_SPECIES
    molasses
    Cr(VI)
    ethanol
    biocide
  END
  IMMOBILE_SPECIES
    biomass
    molasses_im
  END
  MINERALS
    chubbite        # dummy mineral whose volume fraction is 1 - porosity
  END
  REACTION_SANDBOX
    CHROTRAN_PARAMETERS
      NAME_D_MOBILE        molasses
      NAME_D_IMMOBILE      molasses_im
      NAME_C               Cr(VI)
      NAME_B               biomass
      NAME_I               ethanol
      NAME_X               biocide
      NAME_BIOMINERAL      chubbite

      EXPONENT_B           1.0         # alpha [-]

      BACKGROUND_CONC_B    1.e-10      # B_min [mol/m^3_bulk]

      MASS_ACTION_B        0.d0        # Gamma_B [L/mol/s]
      MASS_ACTION_CD       1.0         # Gamma_CD [L/mol/s]
      MASS_ACTION_X        0.d0        # Gamma_X [L/mol/s]

      RATE_B_1             1.d-5       # lambda_B1 [/s]
      RATE_B_2             1.d-6       # lambda_B2 [/s]
      RATE_C               1.d-10      # lambda_C [/s]
      RATE_D               0.d0        # lambda_D [/s]
      RATE_D_IMMOB         150.d-2     # lambda_D_i [/s]
      RATE_D_MOBIL         1.d-2       # lambda_D_m [/s]

      INHIBITION_B         5.d1        # K_B [mol/m^3_bulk]
      INHIBITION_C         1.d-7       # K_C [M]
      MONOD_D              1.d-6       # K_D [M]
      INHIBITION_I         1.d-4       # K_I [M]

      DENSITY_B            1.d20       # [mol/L, i.e., g/L]

      STOICHIOMETRIC_C     0.33d0      # S_C [-]
      STOICHIOMETRIC_D_1   1.d0        # S_D_1 [-]
      STOICHIOMETRIC_D_2   0.020833d0  # S_D_2 [-]
    END
  END
  MINERAL_KINETICS
    chubbite
      RATE_CONSTANT 0.d0
    END
  END
  UPDATE_POROSITY
  MINIMUM_POROSITY 1.d-4
  UPDATE_PERMEABILITY
  DATABASE ./chem.dat
  OUTPUT
    ALL
    FREE_ION
    TOTAL
  END
  LOG_FORMULATION
END
```

Figure A1. Example CHEMISTRY card for CHROTRAN input file. Bold text should not be altered. However, additional species may be added to the PRIMARY_SPECIES, IMMOBILE_SPECIES, MINERALS, and MINERAL_KINETICS blocks, if desired. Additional sandboxes can also be used in the REACTION_SANDBOX block.

```
SIMULATION
  SIMULATION_TYPE SUBSURFACE
  PROCESS_MODELS
    SUBSURFACE_FLOW flow
      MODE RICHARDS
    END
    SUBSURFACE_TRANSPORT transport
      GLOBAL_IMPLICIT
      NUMERICAL_JACOBIAN
    END
  END
END

MATERIAL_PROPERTY soil1
  ID 1
  TORTUOSITY 0.1d0
  PERMEABILITY
    DATASET Permeability
  END
  PERMEABILITY_POWER 1.0
  PERMEABILITY_CRITICAL_POROSITY 0.0
  PERMEABILITY_MIN_SCALE_FACTOR 1.d-4
  CHARACTERISTIC_CURVES cc1
END

CONSTRAINT initial
  CONCENTRATIONS
    molasses    1.d-20 T
    ethanol     1.d-20 T
    biocide     1.d-20 T
    Cr(VI)      1.923d-05 T # 1000 ppb
  END
  IMMOBILE
    biomass     1.d-10  # equal to BACKGROUND_CONC_B
    molasses_im 1.d-20
  END
  MINERALS
    chubbite    0.85 1.0  # 0.85 is initial porosity
  END
```

Figure A2. Additional cards that require particular content in order for CHROTRAN to work properly. In the SIMULATION card, the NUMERICAL_JACOBIAN option must be specified. In the MATERIAL_PROPERTY card, the OPTION PERMEABILITY_MIN_SCALE_FACTOR 1.d4 option should be set. In CONSTRAINT cards, species that are not present should have small, but non-zero concentrations assigned. The concentration of NAME_B (biomass, here) should equal BACKGROUND_CONC_B in the CHEMISTRY CARD. Finally, the initial porosity of the system is set by assigning the volume fraction of NAME_BIOMINERAL (chubbite, here). In general, bold text is required. However, other options may be specified, if desired.

```
'temperature points' 8 0. 25. 60. 100. 150. 200. 250.
'H2O' 3.0 0.0 18.0153
'Cr(VI)' 0. 0. 0.
'molasses' 0. 0. 0.
'ethanol' 0. 0. 0.
'biocide' 0. 0. 0.
'null' 0 0 0
'null' 1 0. '0' 0. 0. 0. 0. 0. 0. 0. 0. 0. 0. 0.
'null' 0. 1 1. '0' 0. 0. 0. 0. 0. 0. 0. 0. 0.
'chubbite' 1.0 0   0. 0. 0. 0. 0. 0. 0. 0. 1.0
'null' 0. 1 0. '0' 0. 0. 0. 0. 0. 0. 0. 0. 0.
'null' 1 0. '0' 0. 0. 0. 0. 0. 0. 0. 0. 0. 0. 0.
```

Figure A3. Minimal CHROTRAN chemistry database. The text shown here should not be removed, however additional species may be added, if desired. See PFLOTRAN user manual for details on the database format.

Table 1. CHROTRAN parameter values used in the bio-fouling example in Section 3.2.

Symbol	Value	Units
α	1	-
$B_{\min}$	10^{-10}	mol m_b^{-3}
Γ_B	2.6×10^{-2}	L mol^{-1} s^{-1}
Γ_{CD}	1	L mol^{-1} s^{-1}
Γ_X	2.6×10^{-5}	L mol^{-1} s^{-1}
λ_{B_1}	10^{-5}	s^{-1}
λ_{B_2}	10^{-15}	s^{-1}
λ_C	10^{-10}	s^{-1}
λ_D	0	s^{-1}
λ_{D_i}	1.5	s^{-1}
λ_{D_m}	10^{-2}	s^{-1}
K_B	5×10^2	mol m_b^{-3}
K_C	10^{-7}	M
K_D	10^{-6}	M
K_I	1	M
ρ_B	10^3	mol L^{-1}
S_C	3.3×10^{-1}	-
S_{D_1}	10^{-5}	-
S_{D_2}	2.0833×10^{-2}	-

These have been corrected to mol L^-1

Table 2. Relationship between the parameter names in the CHEMISTRY card (Figure A1) and the mathematical symbols shown in Section 2.

Symbol	Units	Name in CHEMISTRY card
α	-	EXPONENT_B
$B_{\min}$	mol m_b^{-3}	BACKGROUND_CONC_B
Γ_B	L mol^{-1} s^{-1}	MASS_ACTION_B
Γ_{CD}	L mol^{-1} s^{-1}	MASS_ACTION_CD
Γ_X	L mol^{-1} s^{-1}	MASS_ACTION_X
K_B	mol m_b^{-3}	INHIBITION_B
K_C	mol L^{-1}	INHIBITION_C
K_D	mol L^{-1}	MONOD_D
K_I	mol L^{-1}	INHIBITION_I
λ_{B_1}	s^{-1}	RATE_B_1
λ_{B_2}	s^{-1}	RATE_B_2
λ_C	s^{-1}	RATE_C
λ_D	s^{-1}	RATE_D
λ_{D_i}	s^{-1}	RATE_D_IMMOB
λ_{D_m}	s^{-1}	RATE_D_MOBIL
ρ_B	mol L^{-1}	DENSITY_B
S_C	-	STOICHIOMETRIC_C
S_{D_1}	-	STOICHIOMETRIC_D_1
S_{D_2}	-	STOICHIOMETRIC_D_2